Research Article

Muhammad Jebran Khan, Samina Zuhra, Rashid Nawaz, Balaganesh Duraisamy, Mohammed S. Alqahtani, Kottakkaran Sooppy Nisar*, Wasim Jamshed, and Mohamed Abbas

Numerical analysis of bioconvection-MHD flow of Williamson nanofluid with gyrotactic microbes and thermal radiation: New iterative method

https://doi.org/10.1515/phys-2022-0036
received February 11, 2022; accepted April 11, 2022

Abstract: The aim of this study is to investigate the numerical analysis of an innovative model containing, bioconvection phenomena with a gyrotactic motile microorganism of magnetohydrodynamics Williamson nanofluids flow along with heat and mass transfer past a stretched surface. The effect of thickness variation and thermal conductivity feature is employed in the model. Bioconvection in nanofluid helps in bioscience such as in blood flow, drug delivery, micro-enzyme, biosensors, nanomedicine, for content detection, *etc*. For simulation procedure, the mathematical partial differential equations are converted into dimensionless systems owing to dimensionless variations such as magnetic field, power index velocity, Williamson parameter, wall thickness parameter, thermal conductivity variation, Prandtl number, thermal radiation, Brownian motion, Lewis number, Peclet number, and different concentration parameter, *etc*. For numerical simulation, New Iterative Technique (NIM) numerical algorithm is adopted and employed for the linear regression planned for the proposed model. For comparison purposes, the homotopy technique is employed on the flow model. Close agreement is seen between both methods revealing the accuracy and consistency of NIM numerical technique. Many features of no-scale constraints are evaluated through graphical data for a key profile of the flow model. Results show that microorganism concentration is heavy due to the magnetic effect and Hall current.

Keywords: numerical solution, analysis of bioconvection, MHD, Williamson nanofluid, variable thermal conductivity, variable thickness, numerical iterative method

*** Corresponding author: Kottakkaran Sooppy Nisar,** Department of Mathematics, College of Arts and Sciences, Prince Sattam Bin Abdulaziz University, Wadi Aldawaser, Saudi Arabia, e-mail: n.sooppy@psau.edu.sa
Muhammad Jebran Khan: Department of Mathematics, Lincoln University College, Selangor, Malaysia, e-mail: Jebran.khan@lincoln.edu.my
Samina Zuhra: Department of Computing and Technology, Abasyn University, Peshawar, 25000, Khyber Pakhtunkhwa, Pakistan, e-mail: samina.zuhra@abasyn.edu.pk
Rashid Nawaz: Department of Mathematics, Abdul Wali Khan University Mardan, 23200, Khyber Pakhtunkhwa, Pakistan, e-mail: rashid_uop@yahoo.com
Balaganesh Duraisamy: Department of computer science and multimedia, Faculty of Computer Science and Multimedia, Lincoln University College, Selangor, Malaysia, e-mail: balaganesh@lincoln.edu.my
Mohammed S. Alqahtani: Radiological Sciences Department, College of Applied Medical Sciences, King Khalid University, Abha 61421, Saudi Arabia; BioImaging Unit, Space Research Centre, Michael Atiyah Building, University of Leicester, Leicester, LE1 7RH, United Kingdom, e-mail: mosalqhtani@kku.edu.sa
Wasim Jamshed: Department of Mathematics, Capital University of Science and Technology (CUST), Islamabad, 44000, Pakistan, e-mail: wasiktk@hotmail.com
Mohamed Abbas: Electrical Engineering Department, College of Engineering, King Khalid University, Abha 61421, Saudi Arabia; Computers and Communications Department, College of Engineering, Delta University for Science and Technology, Gamasa 35712, Egypt, e-mail: mabas@kku.edu.sa

Abbreviations

A	stagnation quantity
A^*	coefficient of heat source/sink for space-dependency
B	magnetic field
B^*	coefficient of heat source/sink for temperature-dependency
B_0	constant magnetic field
Cp	specific heat
D_T	thermophoretic diffusion-coefficient
f	dimensionless stream function
K	heat velocity slip factor
k	thermal conductivity $[\mathrm{W(m\,k)^{-1}}]$
k^*	Rosseland mean absorption coefficient $\left[\frac{1}{m}\right]$

$\mathrm{Le} = \frac{\alpha}{D_B}$	Lewis number
$M = \frac{2\sigma B_0^2}{U_0\rho(1+m)}$	elucidated magnetic field
m	flat sheet flow
N	velocity slip
$N\hat{c} = \frac{\rho_p\hat{c}_p}{\rho\hat{c}}(\hat{C}_w - \hat{C}_\infty)$	nanofluid heat capacity
$\mathrm{Nb} = \left(\frac{B_{\hat{T}}\hat{T}_\infty}{D_{\hat{T}}}\right)\frac{(\hat{C}_w - \hat{C}_\infty)}{(\hat{T}_w - \hat{T}_\infty)}$	Brownian diffusivity/thermophoretic diffusivity
Nt	thermophoresis parameter
$\mathrm{Pe} = \frac{bw_c}{D_m}$	Peclet numbers
$\mathrm{Pr} = \frac{v}{\alpha}$	Prandtl number
Q	non-Fourier heat flux
q_r	radiative heat flux
q'''	variable heat source/sink
$\mathrm{Rd} = \frac{4\sigma^\star\hat{T}_\infty^3}{k_\infty k^\star}$	radiation parameter
$\mathrm{Sh}_{\hat{x}} = \frac{Xq_w}{k(\hat{T}_w - \hat{T}_\infty)}$	physical quantities
$S_c = \frac{v}{D_B}$	Schmidt number
T	fluid temperature
T_w	fluid temperature
T_∞	ambient temperature
$u_w = aX$	velocity
V	fluidic velocity
V_w	mass transfer at wall
$\alpha = A\sqrt{\frac{U_0(1+m)}{2v}}$	wall thickness parameter
ε	elucidated magnetic field
ρ	fluid density
$\tilde{u}, \tilde{v}$	velocity components
$\tilde{u}_\infty = a_0X$	velocity of free stream
$\lambda = \hat{T}\sqrt{\frac{U_0^3(\hat{x}+b)^{3m-1}(m+1)}{v}}$	Williamson fluid parameter and thermal conductivity parameter
$\Omega = \frac{N_\infty}{N_w - N_\infty}$	difference in microorganism concentration

1 Introduction

In recent years, researchers have focused on the importance of promoting thermal suspension (size less than 100 nm) of pure liquids such as oil, water (H_2O), glycol, and other nanofluids and small particles. These nanoparticles, such as silver, alumina (Al_2O_3), copper oxide, *etc.*, conduct and regulate heat transfer in freshwater, so these liquids play a vital role in the type of heat carrier in heat exchangers. Choi [1] proposed enhancing the thermal conductivity of fluids with nanoparticles in developments and applications of non-Newtonian flows.

These fluids play important roles in industrial and engineering applications like microelectronics, biomedical equipment, automotive cooling, and energy production. Hay *et al.* [2] discussed the structures of nanofluids in different forms and conditions decline in the production of entropy in nanofluids passing through a thin end under the influence of thermal radiation and the development of entropy is studied under the thermodynamic second law. Salleh *et al.* [3] investigated the the stabilization of the depth axis of the movement of a hydromagnetic fluid on the then narrow and Buongiorno mode is used for Brownian study and thermophoretic interference power in this system. Waini *et al.* [4] discussed uniform heat emission of mixed nanofluids on a flat tip. In this position, the sample measurements were converted into a draught form using sets of other variables and then adjusted the resulting numbers using Mathematica Programming. Gul *et al.* [5] discussed the flow of nanofluids on fine needles for convective nanotubes of fractional order. In the last few years, the debate on the thinning of needles has been very successful. According to Lee [6] and Narain and Uberoi [7], the strength as well as the absence of temperature as the nanofluids pass through a thin vertical needle of cold water is measured. In this expanded work, the authors consider the solution to the problems of metal flow locally and systematically. Chen and Smith [8] discussed heat transfer to a fine needle. In this article, the temperature properties, and the number and volume of the effect of Prandtl to accelerate the uniform flow of water are studied. Van [9] studied the combined flow of a hot needle plate placed on the handles. Finally, various studies have been conducted on water flowing through a good needle using different flow methods [10–15]. Ramesh *et al.* [16] discussed the therapeutic study of the hybrid nanofluid flow in a thin needle using the Darcy-Forchheimer characteristic of the upper package and the outer heat source.

The researcher of this article changed the modeling equation to that of the measurement model and thus changed the response rate to this set of measurement equations. Hamid *et al.* [17] discussed the properties of thermal electrophoresis of a continuously running nanofluid.

The behavior of driving in a nanofluid is explained in two types. One way is recommended by Buongiorno [18], and the other way is recommended by Das and Tiwari [19]. The Buongiorno model consists of more than one inhomogeneous substance in which the flow of pure fluid and nanoparticles is separated from zero. This mode showed more than six different ways to slide the flow of nano drinks. Magnetic fields, Magnus force, Brownian conduction, inertia, drainage, diffusion phosphorylation, and thermophoretic effects are examples of these processes. It has also been mentioned in the work of Buongiorno [18] that of the seven fine methods, only thermophoresis and Brown's diffusion are important for liquids containing nanoparticles. Considering the value of the Buongiorno model, several researchers have successfully applied this model using different geometry and different flow conditions. Over the years, Nield and Kuznetsov [20,21] increased Buongiorno's work. Both authors used the terms "thermophoretic" and "Brownian" and went to great lengths with electrical equations to study the effects of Brownian movement and thermophoresis on these equations by proposing several new scenarios that are on the verge of trouble. Finally, some researchers used the morning image model for flow to apply different types of flow patterns and states. Khan *et al.* [22,23] discussed the Buongiorno's design for the flow of nanoparticles in a series of logs using different water methods. The authors of these studies addressed the hypotheses arising from the results by using appropriate equations and shapeless and partial analysis (homotopy analytical method, HAM) methods. The reader can continue to study the Buongiorno water cycle using a variety of geometry and different flow states in refs. [24–28].

Bioconvection is another fascinating area that has many physical and real-world forms. The movement of an object due to its density gradient on a small, microscopic step is defined as a dynamic change. This density gradient instability is caused by the swimming of microorganisms. This phenomenon usually occurs at the height of the fluid due to the condensation of the fluid in the affected area. Many physicians and procedures require these physical phenomena, such as biofuels, enzymes, micro-systems, biological cells, bacteria, and biotechnology, among others. Biological infection processes fall into different types, such as gyroscopic microorganisms and chemotaxis. and microbes found on land.

This classification depends on the dynamics of many microorganisms. Kuznetsov [29,30] studied biological convection using a large number of nanoparticles. Marikarjuna *et al.* [31] discussed in a vertical kiln, continuous biomarkers of nanoliquids and contracted microorganisms, transforming experimental problems into non-invasive models using a dimensionless variation, and the difference between numerical methods and finite numbers. Uddin *et al.* [32] discussed a mathematical structure for examining the effects of secondary velocity slides on horizontal filter plates. Chebyshev's method was used in this study to get an approximate answer to the problem. The reader can search more for convection oil with different types of water and stream provisions [33–37].

The magnetic field plays an important role in the field of hydrodynamics. The magnetic fields are very important. The term magnetohydrodynamics (MHD) was coined by the Swedish physician Noble Laurat Hannes Alfven. The thermal action and the large amount of MHD over a long period find useful applications in the fields of fiberglass manufacturing, polymer technology, and metallurgy. MHD nano contributes greatly to fluid flow and heat transfer. Akbar *et al.* [38] studied and investigated MHD nanofluidic flow caused by surface tension, compression, and slip effect. Several other studies have addressed the flow of MHD nanowires and recommended effective solutions [39–44]. Nadeem and Hussein [45] observed Williamson's liquid on a rapidly rising surface and examined the heat transfer. Waheed [46] discussed mixed sensory heat transfer in rectangular containers guided by continuous horizontal plates. Acharya *et al.* [47] proposed unsteady bioconvective squeezing flow with higher-order chemical reaction and second-order slip effects. Acharya [48] studied spectral quasi linearization simulation on the radiative nanofluid spraying over a permeable inclined spinning disk considering the existence of a heat source/sink. Acharya *et al.* [49] studied spectral quasi linearization simulation of radiative nanofluidic transport over a bent surface considering the effects of multiple convective conditions. Shah *et al.* [50] investigated numerical modeling on hybrid nanofluid (Fe_3O_4 + MWCNT/H_2O) migration considering MHD effect over a porous cylinder. Shah *et al.* [51] discussed the simulation of entropy optimization and thermal behavior of nanofluid through the porous media. Shah *et al.* [52] studied the impact of nanoparticle shape and radiation on the behavior of nanofluids under the Lorentz forces. Bilal *et al.* [53] investigated unsteady hybrid-nanofluid flow comprising ferrous oxide and CNTs through a porous horizontal channel with dilating/squeezing walls. Marzougui *et al.* [54] discussed entropy generation on the magneto-convective flow of copper–water nanofluid in a cavity with chamfers.

In 2006, a new method was developed called the new iterative method (NIM) for linear and nonlinear functional equations by Daftardar-Gejji and Jafari [55]. The fixed method operates linear and non-linear classifications in a straightforward polynomial way in nonlinear terms such as ADM. The need for the Lagrange function increases with its algorithm, such as VIM, and the need for route choice of route numbers. The judiciary is free from a small intellectual parliament, in contrast to the judicial tribunal. Since NIM is an iterative method, it needs the first condition to become its main value. Subsequently, the method was developed by many analysts for different problems, including algebraic equations, change equations, common and varied equations, and a system of non-linear measurement equations. Daftardar-Gejji and Bhalekar [56] discussed that lines tested with non-linear separation equilibrium equations terminate domains with the Dirichlet boundary conditions using a new repeating method. String and non-linear separation-wave equations were analyzed using the iterative method developed by Daftardar-Gejji and Bhalekar [57]. Bhalekar and Daftardar-Gejji [58] evaluated a separate component of effective use using a new iterative method. Bhalekar and Daftardar-Gejji [59] used the hypothetical method of control, which is complete in the context of the conversion of that method of decay. The new iterative approach was used to address the nth-command lines and non-linear integral-differentiation equations by Hemeda [60]. The Newell–Whitehead–Segel equation was investigated using NIM by Yaseen and Samraiz [61]. Patade and Bhalekar [62] showed an iterative method for correcting unequal equations that include only the first design function. A family of repeated regression models in which the system of linear equations was presented by Noor and Noor [63]. Noor *et al.* [64] promoted and evaluated alternative design relationships that create different classes of iterative behaviors for the informal investigation of problems using a combined simulation system. Shah and Noor [65] discussed the higher order iteration method for non-linear equations with decomposition technique.

2 Problem formulation

Considered a two dimensional, incompressible, hydromagnetic flow of Williamson nanofluid present across a horizontal stretching surface. A slit point is assumed in the center from which the surface is drawn in a fluid medium. The flow is assumed under the effect of thermal radiative flux and bioconvection with gyrotactic microorganisms. The Cartesian coordinate x-axis is in the stretchable sheet direction with the velocity $\hat{u}_w = \hat{u}_0(\hat{x} + b)^m$ whereas y-axis lies in the normal direction of the stretchable sheet surface. Assume that the thickness of the surface is variable according to $\hat{y} = A(\hat{x} + b)^{\frac{1-m}{2}}$, where $A \geq 0$ indicates the constant of the surface and m is the velocity power index. Assume T_w and C_w are the wall temperature and concentration which are higher than the ambient temperature T_∞ and concentration C_∞ far away. The nanofluid is considered to not influence the way of swimming of microorganisms and their velocity. Magnetic field is exerted in y-axis direction of strength B with a low Reynolds number. Figure 1 shows the flow model configuration.

The mathematical expressions for mass, momentum, energy, nanofluid, and microorganism concentration are as follows:

$$\frac{\partial \hat{u}}{\partial \hat{x}} + \frac{\partial \hat{u}}{\partial \hat{y}} = 0, \tag{1}$$

$$\hat{u}\left(\frac{\partial \hat{u}}{\partial \hat{x}}\right) + v\left(\frac{\partial \hat{u}}{\partial \hat{y}}\right) = v\left(\frac{\partial^2 \hat{u}}{\partial \hat{y}^2}\right) - \frac{\sigma B^2}{\rho}\hat{u} + 2^{1/2} v \Gamma \left(\frac{\partial \hat{u}}{\partial \hat{y}}\right)\left(\frac{\partial^2 \hat{u}}{\partial \hat{y}^2}\right), \tag{2}$$

$$\hat{u}\left(\frac{\partial \hat{T}}{\partial \hat{x}}\right) + v\left(\frac{\partial \hat{T}}{\partial \hat{y}}\right) = \frac{1}{\rho \hat{c}_p}\frac{\partial}{\partial \hat{y}}\left(k\frac{\partial \hat{T}}{\partial \hat{y}}\right) - \frac{1}{\rho \hat{c}_p}\left(\frac{\partial q_r}{\partial \hat{y}}\right) + \frac{\rho \hat{c}_p}{p\hat{c}_f}\left(D_B \frac{\partial \hat{C}}{\partial \hat{y}}\frac{\partial \hat{T}}{\partial \hat{y}} + \frac{D_{\hat{T}}}{\hat{T}_\infty}\left(\frac{\partial \hat{T}}{\partial \hat{y}}\right)^2\right), \tag{3}$$

$$\hat{u}\left(\frac{\partial \hat{C}}{\partial x}\right) + v\left(\frac{\partial \hat{C}}{\partial \hat{y}}\right) = \frac{D_{\hat{T}}}{\hat{T}_\infty}\left(\frac{\partial^2 \hat{T}}{\partial \hat{y}^2}\right) + D_B\left(\frac{\partial^2 \hat{C}}{\partial \hat{y}^2}\right), \tag{4}$$

$$\hat{u}\left(\frac{\partial \hat{N}}{\partial \hat{x}}\right) + \hat{v}\left(\frac{\partial \hat{N}}{\partial \hat{y}}\right) + \frac{bW_c}{\hat{C}_w - \hat{C}_\infty}\left(\frac{\partial \hat{N}}{\partial \hat{y}}\frac{\partial \hat{C}}{\partial \hat{y}} + \hat{N}\frac{\partial^2 \hat{C}}{\partial \hat{y}^2}\right) = D_m\left(\frac{\partial^2 \hat{N}}{\partial \hat{y}^2}\right). \tag{5}$$

The corresponding boundary conditions are:

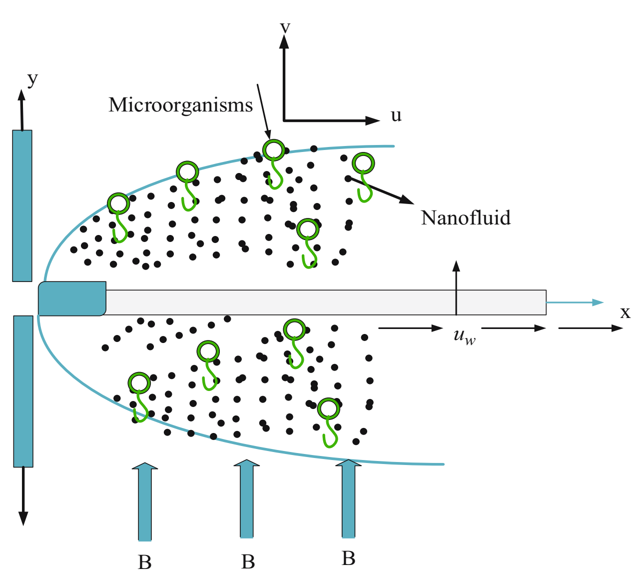

Figure 1: Geometry of microorganism nanofluids model.

$$\begin{cases} \hat{u} = \hat{u}_w(\hat{x}) = \hat{U}_0(\hat{x} + b)^m, \\ \hat{v} = 0, \\ \hat{T} = \hat{T}_w, & \text{for } \hat{y} = (\hat{x} + b)^{\frac{1-m}{2}} \\ \hat{C} = \hat{C}_w, \\ \hat{N} = \hat{N}_w, \end{cases} \tag{6}$$

$$\text{and} \begin{cases} \hat{u} = 0, \\ \hat{T} = \hat{T}_\infty, \\ \hat{C} = \hat{C}_\infty, \\ \hat{N} = \hat{N}_\infty \end{cases} \text{for } \hat{y} = \infty.$$

Roseland approximation for radiation is defined by

$$q_r = -\frac{4\sigma^*}{3k^*}\left(\frac{\partial \hat{T}^4}{\partial \hat{y}}\right), \tag{7}$$

where extending the Taylor series at temperature $\hat{T}_\infty$ with ignoring higher order of $\hat{T}_\infty$ as,

$$\hat{T}^4 = 4\hat{T}_\infty^4 \hat{T} - 3\hat{T}_\infty^4. \tag{8}$$

By utilizing Eqs. (7) and (8), we set:

$$\frac{\partial q_r}{\partial \hat{y}} = -\left(\frac{16\sigma^* \hat{T}_\infty^3}{3k^*}\right)\left(\frac{\partial^2 \hat{T}}{\partial \hat{y}^2}\right). \tag{9}$$

2.1 Transformation to ordinary differential equations (ODEs) system

To solve the mathematical expression of mass, momentum, energy, nanofluid concentration, and motile microorganism concentration Eqs. (1–6), suitable similarity transformations have been adopted that convert these partial differential equation (PDE) systems into simple ODEs which satisfy the mass equation.

Transformation variables are as follow:

$$\begin{aligned} \eta &= \sqrt{\frac{\hat{U}_0(m-1)}{2v}}\left(\hat{y}\,(\hat{x} + b)^{\frac{m-1}{2}} - A\right), \\ \psi &= \sqrt{\frac{2v\hat{U}_0}{m+1}}(\hat{x} + b)^{\frac{m+1}{2}} f(\eta), \\ \theta(\eta) &= \frac{\hat{T} - \hat{T}_\infty}{\hat{T}_w - \hat{T}_\infty}, \ \phi(\eta) = \frac{\hat{C} - \hat{C}_\infty}{\hat{C}_w - \hat{C}_\infty}, \\ \chi(\eta) &= \frac{\hat{N} - \hat{N}_\infty}{\hat{N}_w - \hat{N}_\infty}. \end{aligned} \tag{10}$$

Here Eq. (1) is true identically, while Eqs. (2–5) have the forms:

$$f''' + \lambda f'' f''' + f f'' - \left(\frac{2m}{m+1}\right)(f')^2 - Mf' = 0, \tag{11}$$

$$\begin{aligned} &(1 + 0.75\mathrm{Rd})(1 + \varepsilon\theta + \theta'' + \varepsilon(\theta')^2) \\ &\quad + \Pr f\theta' + \frac{\mathrm{Nc}}{\mathrm{Le}}\phi'\theta' + \frac{\mathrm{Nc}}{\mathrm{Le\,Nb}}(\theta')^2 = 0, \end{aligned} \tag{12}$$

$$\phi'' + \mathrm{Le}\Pr f\phi' + \frac{1}{\mathrm{Nb}}\theta'' = 0, \tag{13}$$

$$\chi'' + 2\sqrt{\frac{m+1}{m-1}}\,\mathrm{Sc}\, f\chi' - \mathrm{Pe}(\chi\phi' + \chi\phi'' + \Omega\phi'') = 0. \tag{14}$$

The corresponding boundary conditions

$$\begin{cases} f'(0) = 1, \\ f(0) = \alpha\left(\frac{1-m}{1+m}\right), \\ \theta(0) = 1, & \text{at } \eta = 0, \\ \phi(0) = 1, \\ \chi(0) = 1, \end{cases} \tag{15}$$

$$\text{and} \begin{cases} f'(\infty) = 0, \\ \theta(\infty) = 0, \\ \phi(\infty) = 0, \\ \chi(\infty) = 0. \end{cases} \text{at } \eta = \infty.$$

3 Numerical solution of ODE systems

A suitable numerical method is too much necessary for the computational of fluidic problems. Here we use a new iterative technique to solve the ODE systems in Eqs. (11–15).

3.1 Basic principles of the NIM

The new iterative method (NIM) is enlightened in this sub-section (see, [55]). Let us consider the following differential equation

$$\hat{W}(\eta) = L(\hat{W}(\eta)) + \hat{g}(\eta) + \hat{N}(\hat{W}(\eta)).$$

According to our model

$$\begin{cases} \hat{f}(\eta) = L(\hat{f}(\eta) + \hat{g} + \hat{N}(\hat{f}(\eta)), \\ \hat{\theta}(n) = L(\hat{\theta}\hat{f}(\eta) + \hat{g}(\eta) + \hat{N}(\hat{\theta}(\eta)), \\ \hat{\varphi}(\eta) + L(\hat{\varphi}\hat{f}(\eta) + \hat{g}(\eta) + \hat{N}(\hat{\varphi}(\eta)), \\ \hat{\chi}(\eta) = L(\hat{\chi}(\eta)) + \hat{g}(\eta) + \hat{N}(\hat{\chi}(\eta)). \end{cases} \tag{16}$$

For a linear factor is indicated by L, $\hat{g}(\eta)$ is a known function and $\hat{W}(\eta)$ is an unknown function. Suppose that the solution of the new iterative method of Eq. (16) is of the form

$$\hat{W}(\eta) = \sum_{i=0}^{\infty} \hat{W}_i. \tag{17}$$

For the function of the proposed model, Eq. (17) can be formed as,

$$\hat{f}(\eta) = \sum_{i=o}^{\infty}\hat{f}_i,\quad \hat{\theta}(\eta) = \sum_{i=o}^{\infty}\hat{\theta}_i,$$
$$\hat{\varphi}(\eta) = \sum_{i=o}^{\infty}\hat{\varphi}_i,\quad \hat{\chi}(\eta) = \sum_{i=o}^{\infty}\hat{\chi}_i.$$

As $\hat{L}$ is a linear operator, therefore

$$\hat{L}\left(\sum_{i=0}^{\infty}\hat{W}_i\right) = \sum_{i=0}^{\infty}\hat{f}_i + \sum_{i=0}^{\infty}\theta_i + \sum_{i=0}^{\infty}\varphi_i + \sum_{i=0}^{\infty}\hat{x}_i. \tag{18}$$

The non-linear operator is given by ref. [47].

$$\begin{aligned}\hat{N}\left(\sum_{i=0}^{\infty}\hat{W}_i\right) &= \hat{N}(\hat{W}_0) + \sum_{i=1}^{\infty}\left\{\hat{N}\left(\sum_{j=0}^{i}\hat{W}_j\right) - \hat{N}\left(\sum_{j=0}^{i-1}\hat{W}_j\right)\right\}\\ &= \sum_{i=0}^{\infty}E_i,\end{aligned} \tag{19}$$

Here

$$\begin{cases}\hat{N}\left(\sum_{i=0}^{\infty}\hat{f}_i\right) = \hat{N}(\hat{f}_0) + \sum_{i=1}^{\infty}\left\{\hat{N}\left(\sum_{j=0}^{i}\hat{f}_j\right) - \hat{N}\left(\sum_{j=0}^{i-1}\hat{f}_j\right)\right\} = \sum_{i=0}^{\infty}E_{1i},\\ \hat{N}\left(\sum_{i=0}^{\infty}\hat{\theta}_i\right) = \hat{N}(\hat{\theta}_0) + \sum_{i=1}^{\infty}\left\{\hat{N}\left(\sum_{j=0}^{i}\hat{\theta}_j\right) - \hat{N}\left(\sum_{j=0}^{i-1}\hat{\theta}_j\right)\right\} = \sum_{i=0}^{\infty}E_{2i},\\ \hat{N}\left(\sum_{i=0}^{\infty}\hat{\varphi}_i\right) = \hat{N}(\hat{\varphi}_0) + \sum_{i=1}^{\infty}\left\{\hat{N}\left(\sum_{j=0}^{i}\hat{\varphi}_j\right) - \hat{N}\left(\sum_{j=0}^{i-1}\hat{\varphi}_j\right)\right\} = \sum_{i=0}^{\infty}E_{3i},\\ \hat{N}\left(\sum_{i=0}^{\infty}\hat{\chi}_i\right) = \hat{N}(\hat{\chi}_0) + \sum_{i=1}^{\infty}\left\{\hat{N}\left(\sum_{j=0}^{i}\hat{\chi}_j\right) - \hat{N}\left(\sum_{j=0}^{i-1}\hat{\chi}_j\right)\right\} = \sum_{i=0}^{\infty}E_{4i},\end{cases}$$

where $E_0 = \hat{N}(\hat{W}_0)$ and

Table 2: Numerical technique *vs* analytical solution for temperature profile

η	NIM	HAM	Absolute error
0.0	1.00628	1.00	0.00628196
0.5	0.52617	0.606531	0.0803606
1.0	0.300561	0.367879	0.0673187
1.5	0.178216	0.22313	0.0449137
2.0	0.107204	0.135335	0.0281313
2.5	0.0648315	0.082085	0.0172535
3.0	0.0392825	0.0497871	0.0105046
3.5	0.0238181	0.0301974	0.00637925
4.0	0.014445	0.0183156	0.0038706
4.5	0.00876119	0.011109	0.00234781
5.0	0.00531394	0.00673795	0.00142401

Table 3: Numerical technique *vs* analytical solution for nanofluid concentration profile

η	NIM	HAM	Absolute error
0.0	1.00268	1.00002	0.002656
0.5	0.599198	0.606542	0.00734398
1.0	0.360821	0.367885	0.00706385
1.5	0.218048	0.223133	0.00508493
2.0	0.131995	0.135337	0.00334216
2.5	0.0799723	0.0820861	0.00211377
3.0	0.0484756	0.0497877	0.00131208
3.5	0.0293913	0.0301978	0.000806442
4.0	0.0178229	0.0183159	0.000492947
4.5	0.0108088	0.0111091	0.00030037
5.0	0.00655534	0.00673803	0.000182688

Table 1: Numerical technique *vs* analytical solution for velocity profile

η	NIM	HAM	Absolute error
0.0	1.00000	1.00000	1.25608×10^{-6}
0.5	0.616065	0.616119	0.0000534592
1.0	0.376676	0.376915	0.000239218
1.5	0.229501	0.229725	0.000223707
2.0	0.139570	0.139729	0.000159905
2.5	0.0847875	0.0848917	0.000104138
3.0	0.0514753	0.0515406	0.0000653048
3.5	0.0312394	0.0312797	0.0000402754
4.0	0.0189543	0.0189789	0.0000246443
4.5	0.0114988	0.0115138	0.0000150203
5.0	0.00697525	0.00698438	9.13554×10^{-6}

Table 4: Numerical technique *vs* analytical solution for nanofluid concentration profile

η	NIM	HAM	Absolute error
0.0	1.00884	0.999987	0.00885519
0.5	0.611377	0.606524	0.00485344
1.0	0.370617	0.367876	0.00274073
1.5	0.224751	0.223129	0.00162255
2.0	0.136317	0.135335	0.000982388
2.5	0.0826835	0.0820848	0.000598777
3.0	0.0501521	0.049787	0.000365143
3.5	0.0304197	0.0301973	0.000222405
4.0	0.0184509	0.0183156	0.000135288
4.5	0.0111912	0.011109	0.0000822121
5.0	0.00678786	0.00673794	0.0000499239

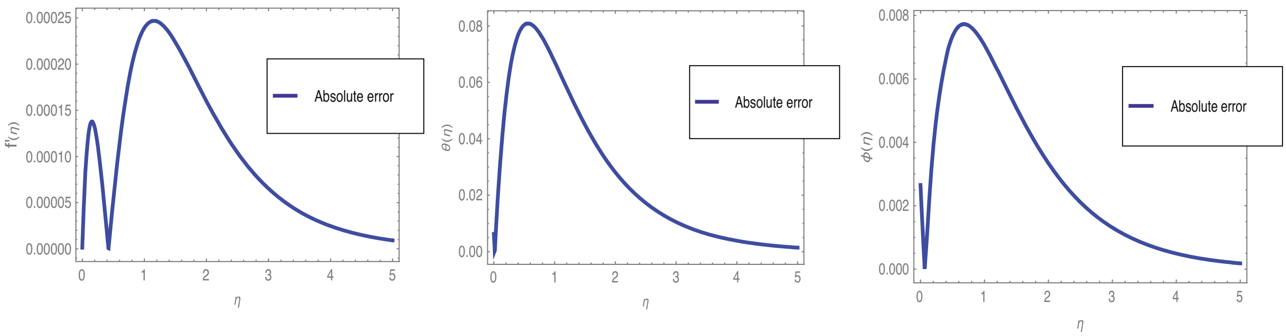

Figure 2: Absolute errors for the velocity, temperature, and concentration profile.

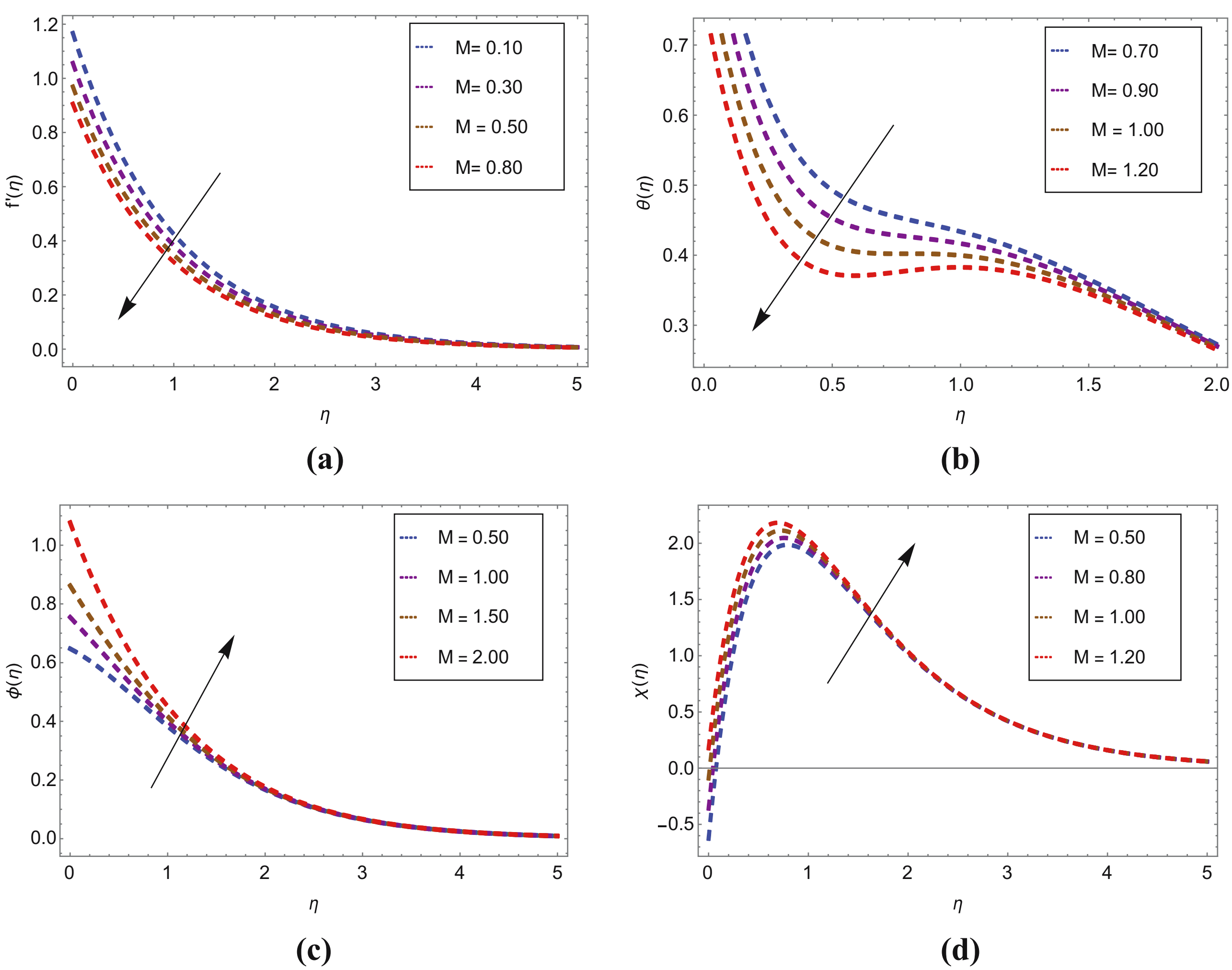

Figure 3: Consequences of magnetic parameter on: (a) velocity profile, (b) temperature gradient, (c) nanofluid concentration, and (d) motile microorganism concentration.

$$E_i = \left\{\hat{N}\left(\sum_{j=0}^{i}\hat{W}_j\right) - \hat{N}\left(\sum_{j=0}^{i-1}\hat{W}_j\right)\right\}, \tag{20}$$

Here

$$E_{1i} = \left\{\hat{N}\left(\sum_{j=0}^{i}\hat{f}_j\right) - \hat{N}\left(\sum_{j=0}^{i-1}\hat{f}_j\right)\right\},$$

$$E_{2i} = \left\{\hat{N}\left(\sum_{j=0}^{i}\hat{\theta}_j\right) - \hat{N}\left(\sum_{j=0}^{i-1}\hat{\theta}_j\right)\right\},$$

$$E_{3i} = \left\{\hat{N}\left(\sum_{j=0}^{i}\hat{\varphi}_j\right) - \hat{N}\left(\sum_{j=0}^{i-1}\hat{\varphi}_j\right)\right\},$$

$$E_{4i} = \left\{\hat{N}\left(\sum_{j=0}^{i}\hat{\chi}_j\right) - \hat{N}\left(\sum_{j=0}^{i-1}\hat{\chi}_j\right)\right\}.$$

Substituting Eqs. (18–20) in Eq. (16) we obtain

$$\sum_{i=0}^{\infty}\hat{W}_i = \hat{g}(\eta) + \sum_{j=0}^{i}\hat{L}(\hat{W}_j) + \sum_{i=0}^{\infty}E_i. \tag{21}$$

The final form of the model is as follows,

$$\sum_{i=0}^{\infty}\hat{f}_i = \hat{g}(\eta) + \sum_{j=0}^{i}\hat{L}(\hat{f}_j) + \sum_{i=0}^{\infty}E_{1i},$$

$$\sum_{i=0}^{\infty}\hat{\theta}_i = \hat{g}(\eta) + \sum_{j=0}^{i}\hat{L}(\hat{\theta}_j) + \sum_{i=0}^{\infty}E_{2i},$$

$$\sum_{i=0}^{\infty}\hat{\varphi}_i = \hat{g}(\eta) + \sum_{j=0}^{i}\hat{L}(\hat{\varphi}_j) + \sum_{i=0}^{\infty}E_{3i},$$

$$\sum_{i=0}^{\infty}\hat{\chi}_i = \hat{g}(\eta) + \sum_{j=0}^{i}\hat{L}(\hat{\chi}_j) + \sum_{i=0}^{\infty}E_{4i}.$$

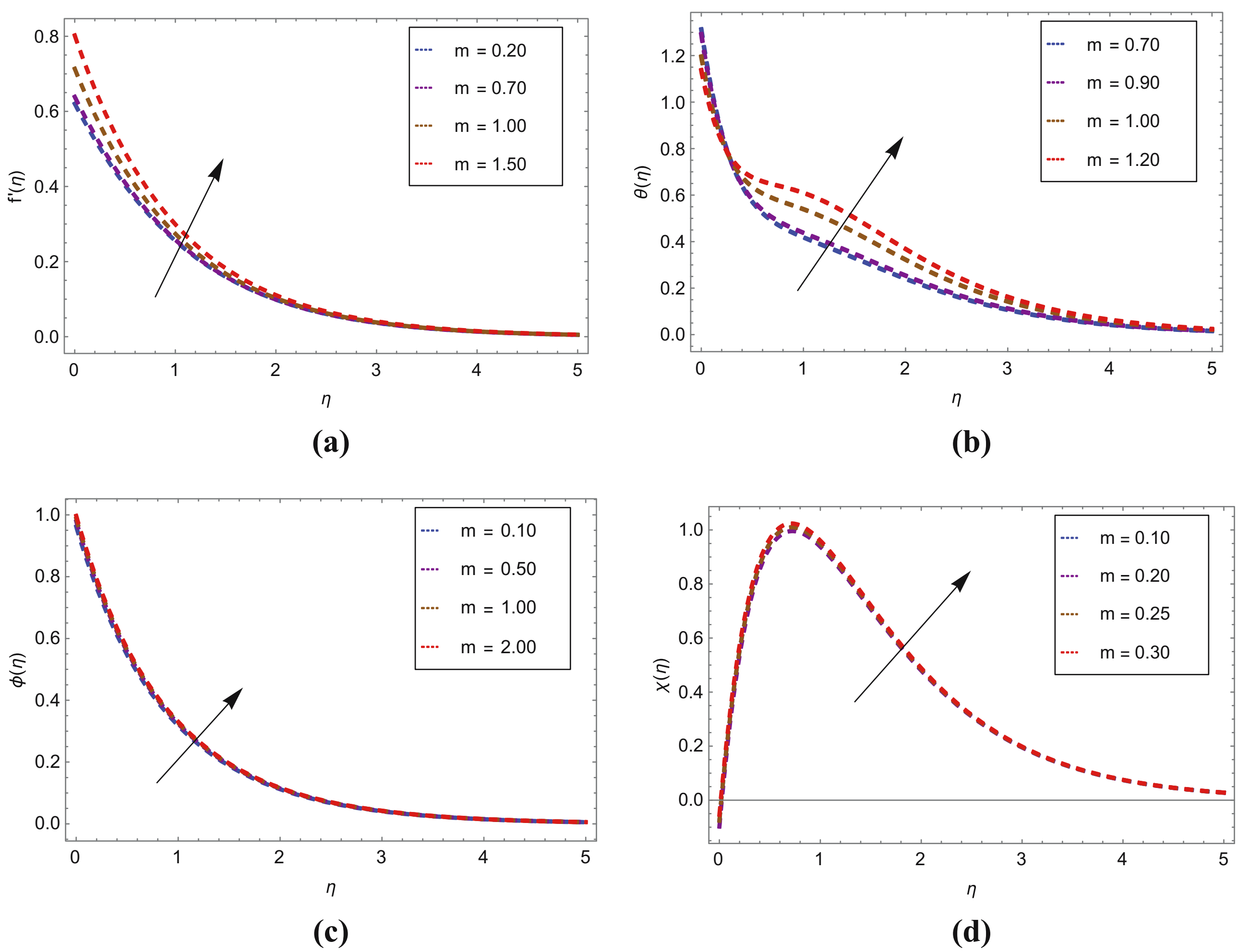

Figure 4: Consequences of velocity power index on: (a) velocity profile, (b) temperature gradient, (c) nanofluid concentration, and (d) motile microorganism concentration.

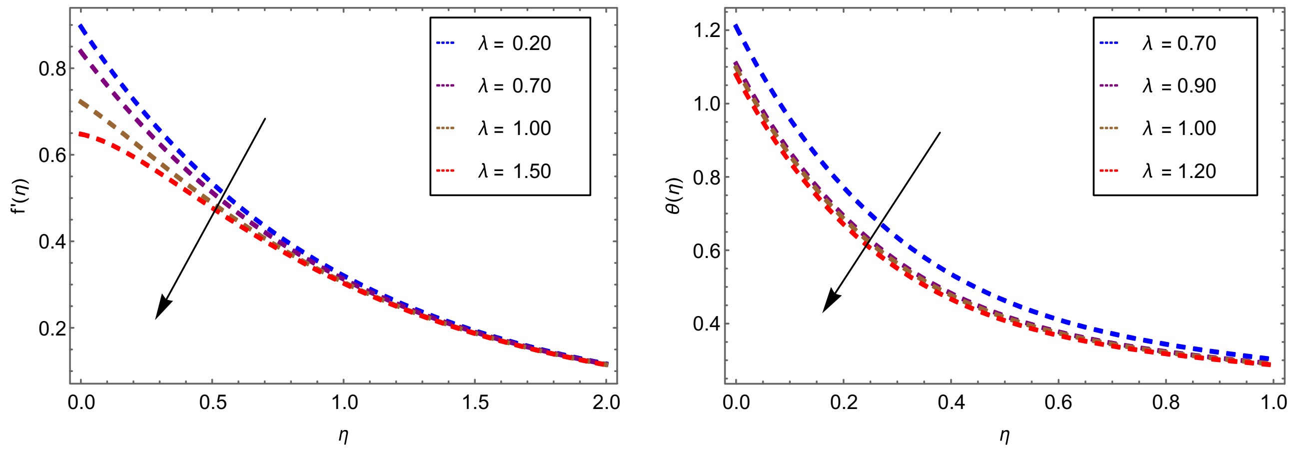

(a) (b)

Figure 5: Consequences of Williamson parameter on: (a) velocity profile and (b) temperature gradient.

3.2 Comparison of NIM with HAM

Computational outcomes of Eqs. (11–15) is achieved *via* a new iterative technique and HAM. Excellent agreement between numerical and analytical solutions reveals the significance mode of NIM. Both methods' comparison and their residual errors are expressed in Tables 1–4 and Figures 2–5. A falling tendency in average squared residual error is detected for higher-order deformations. Average residual errors for all computational outcomes ranging from 10^{-3} to 10^{-6} show that NIM is reliable and asymptotically convergent for fluidic problems.

4 Results and discussion (interpretation of variations)

Demonstrates characteristics of variations such as magnetic field M, power index velocity m, Williamson parameter λ, wall thickness parameter α, thermal conductivity variation ε, Prandtl number Pr, thermal radiation Rd, Brownian motion Nb, Peclet number Pe, and different concentration parameter Ω against velocity profile $f'(\eta)$, temperature distribution $\theta(\eta)$, solutal nanoparticles distribution $\phi(\eta)$, and concentration of motile microorganism distribution $\chi(\eta)$ of Eqs. (11–14) with boundary conditions,

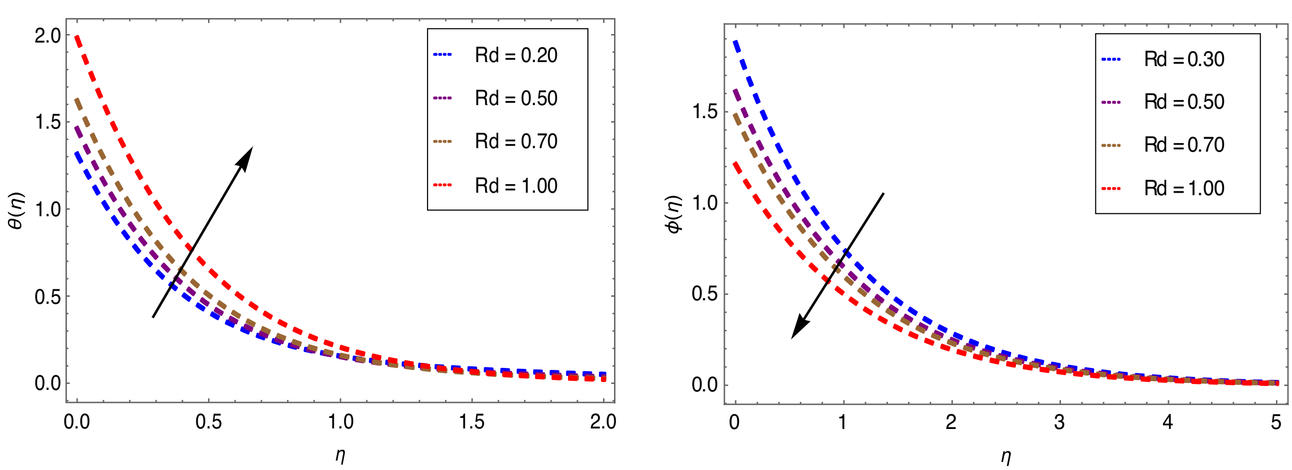

(a) (b)

Figure 6: Consequences of thermal radiation parameter on: (a) velocity profile and (b) temperature gradient.

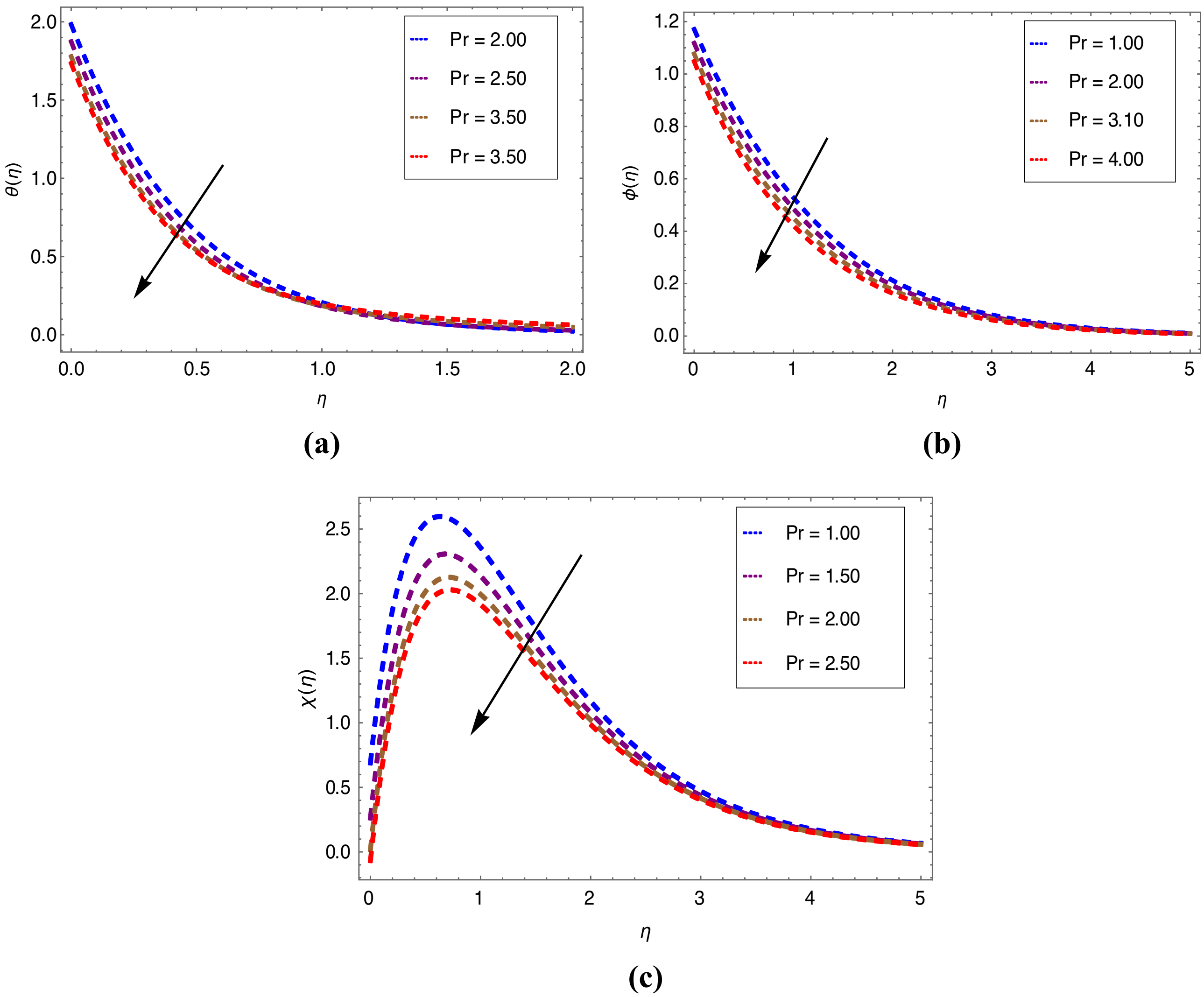

Figure 7: Consequences of Prandtl number on: (a) temperature gradient, (b) nanofluid concentration, and (c) motile microorganism concentration.

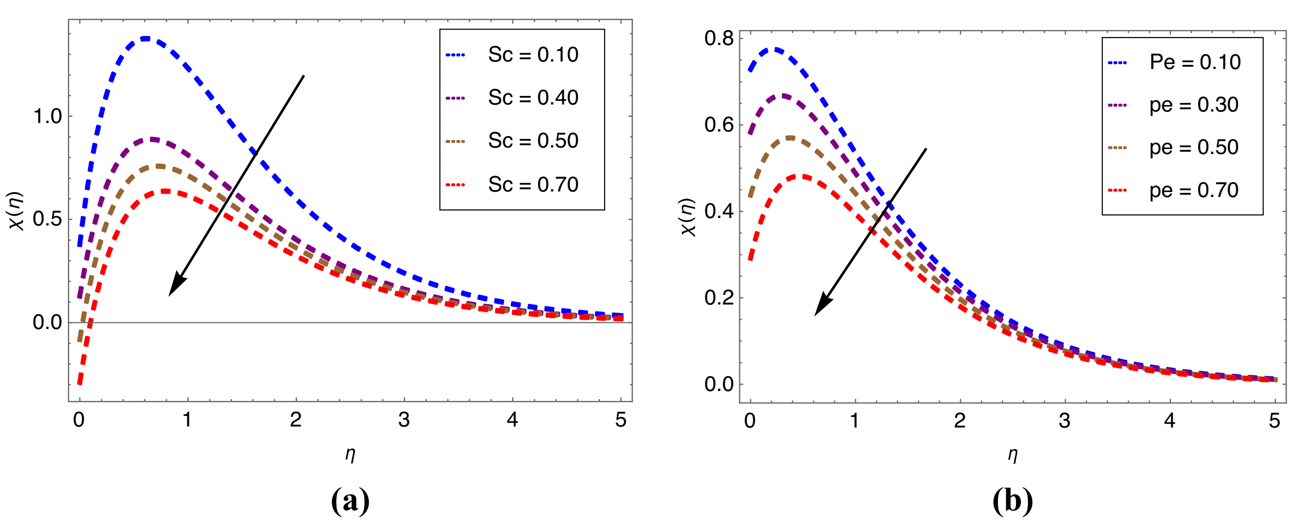

Figure 8: Consequences of (a) Schmidt number, (b) Peclet number on motile microorganism concentration profile.

Eq. (15) is analyzed in Figures 3–8. Properties of magnetic field effects M on the velocity, temperature, solutal, and microorganism concentration fields are described in Figure 3. Lorentz force is the force that a magnetic field exerts on a moving electric charge. The fluid viscosity increases due to the Lorentz force characteristic in the magnetic field, thereby reducing the velocity profile and temperature gradient as well, as shown in Figure 3(a and b), whereas Figure 3(c and d) dispatch the strong concentration behavior of nanofluid and microorganisms when the viscosity created by magnetic force increases. As the name shows, velocity power index m speeds up the momentum boundary layer thickness and thermal boundary layer thickness when the values of m vary. This causes the stability in diluted distribution of nanofluid and swimming microorganisms (Figure 4). A non-Newtonian fluid does not obey Newton's law of viscosity, which states that viscosity should remain constant regardless of stress. In non-Newtonian fluids, viscosity can alter when subjected to force, becoming either more liquid or more solid. When shaken, ketchup, for example, gets runnier, making it a non-Newtonian fluid. Williamson parameter possesses the viscoelastic shear thinning characteristic of non-Newtonian fluid. The higher the non-Newtonian Williamson parameter, the greater the thickness of the boundary layer. In Figure 5, the flow rate and temperature distribution upsurge for a greater value of Williamson quantity. Thermal radiation refers to electromagnetic radiation that generates energy, which is emitted by a heated surface in all dimensions. Enhancing the thermal radiation parameter enhances the energy field but the higher electromagnetic radiation decreased the diluted concentration of Williamson nanofluid (Figure 6). Prandtl quantity is essential for the fluidic problem as it sets the fluid viscosity in correlation with thermal conductivity. Figure 7 displays the opposite impact of Prandtl number against the temperature field, concentration, and swimming microorganism profile. It controls the momentum thickness and thermal boundary layer; hence, the greater the Pr, the lesser the thermal boundary layer thickness. Figure 8(a) shows the Schmidt quantity (in a chemical process, it describes the hydrodynamic impact of the flowing fluid's inertia and friction forces) against the microorganism concentration profile. It is the ratio of kinematic viscosity to microorganism molecular diffusivity. Elevation in kinematic viscosity (a value that represents a fluid's dynamic viscosity per unit density) restricts the movement of motile microbes. To slow down this movement, Schmidt parameter is increased. Figure 8(b) shows the decreasing behavior of the density of microorganisms against the Peclet number, which is the study of transportation in the swimming continuum of microorganisms defined as maximum motile microbes' swimming speed *vs* microbes' diffusion rate (the quantity of diffusing molecules inside cell changes throughout time). Microbe's diffusion is the movement of motile from a highly concentrated area to a lower concentration in the light of gyrotactic.

5 Conclusion

This study makes various aspects of heat transfer and radiation effects on hydromagnetic boundary layer Williamson nanofluid flow via a new iterative technique. With few iterations, the correlation with the HAM is ranging from 10^{-6} to 10^{-3}, which proves that the proposed technique is reliable, accurate, and rapid convergent for fluidic problems.

Additionally, the effects of the variations are highlighted as:

- Flow rate upsurges for Hall current parameter and wall thickness quantity whereas it slows down for the increase in the range of the magnetic parameter and Williamson quantity.
- Temperature distribution rises for Hall current parameter, wall thickness quantity, thermal conductivity parameter, and thermal radiation quantity but it has opposite fluctuation against the Prandtl number, magnetic force, Williamson quantity, and Lewis number.
- Nanofluidic concentration has direct correlation with magnetic quantity, Hall current quantity, Williamson parameter, and thermal conductivity whereas the behavior of Lewis number and thermal radiation is seen to oppose this profile.
- The Bioconvection microorganism concentration field goes fast in the presence of the magnetic field, Hall current parameter, and wall thickness quantity but it becomes slow for the higher value of Prandtl number, Schmidt number and Peclet number.

Acknowledgments: The authors extend their appreciation to the Deanship of Scientific Research at King Khalid University (KKU) for funding this research project Number (R.G.P1./92/40).

Funding information: Deanship of Scientific Research at King Khalid University (KKU) (R.G.P1./92/40).

Author contributions: All authors have accepted responsibility for the entire content of this manuscript and approved its submission.

Conflict of interest: The authors state no conflict of interest.

References

[1] Choi SUS. Enhancing thermal conductivity of fluids with nanoparticles. In: Siginer DA, Wang HP, editors. Developments and applications of non-newtonian flows, FED. Vol. 231/MD-Vol. 66. New York: ASME; 1995. p. 99–105.
[2] Khan MWA, Khan MI, Hayat T, Alsaedi A. Entropy generation minimization (EGM) of nanofluid flow by a thin moving needle with nonlinear thermal radiation. Phys B. 2018;534:113–9.
[3] Salleh SNA, Bachok N, Arifin NM, Ali FM, Pop I. Magnetohydrodynamics flow past a moving vertical thin needle in a nanofluid with stability analysis. Energies. 2018;11(12):3297.
[4] Waini I, Ishak A, Pop I. Hybrid nanofluid flow and heat transfer past a vertical thin needle with prescribed surface heat flux. Int J Numer Methods Heat Fluid Flow. 2019;29(12):4875–94.
[5] Gul T, Khan M, Noman W, Khan I, Abdullah Alkanhal T, Tlili I. Fractional order forced convection carbon nanotube nanofluid flow passing over a thin needle. Symmetry. 2019;11(3):312.
[6] Lee LL. Boundary layer over a thin needle. Phys Fluids. 1967;10(4):820–2.
[7] Narain JP, Uberoi MS. Combined forced and free-convection heat transfer from vertical thin needles in a uniform stream. Phys Fluids. 1972;15(11):1879–82.
[8] Chen JLS, Smith TN. Forced convection heat transfer from nonisothermal thin needles. J Heat Transf. 1978;100(2):358–62. doi: 10.1115/1.3450809.
[9] Wang CY. Mixed convection on a vertical needle with heated tip. Phys Fluids A. 1990;2(4):622–5.
[10] Souayeh B, Reddy MG, Sreenivasulu P, Poornima T, Rahimi-Gorji M, Alarifi IM. Comparative analysis on non-linear radiative heat transfer on MHD Casson nanofluid past a thin needle. J Mol Liq. 2019;284:163–74.
[11] Ahmad S, Arifin NM, Nazar R, Pop I. Mixed convection boundary layer flow along vertical thin needles: Assisting and opposing flows. Int Commun Heat Mass Transf. 2008;35(2):157–62.
[12] Mabood F, Nayak MK, Chamkha AJ. Heat transfer on the cross flow of micropolar fluids over a thin needle moving in a parallel stream influenced by binary chemical reaction and Arrhenius activation energy. Eur Phys J Plus. 2019;134(9):427.
[13] Khan I, Khan WA, Qasim M, Afridi I, Alharbi SO. Thermodynamic analysis of entropy generation minimization in thermally dissipating flow over a thin needle moving in a parallel free stream of two Newtonian fluids. Entropy. 2019;21(1):74.
[14] Hamid A. Terrific effects of Ohmic-viscous dissipation on Casson nanofluid flow over a vertical thin needle: buoyancy assisting & opposing flow. J Mark Res. 2020;9(5):11220–30.
[15] Tlili I, Nabwey HA, Reddy MG, Sandeep N, Pasupula M. Effect of resistive heating on incessantly poignant thin needle in magnetohydrodynamic Sakiadis hybrid nanofluid. Ain Shams Eng J. 2021;12(1):1025–32. doi: 10.1016/j.asej.2020.09.009.
[16] Ramesh GK, Shehzad SA, Izadi M. Thermal transport of hybrid liquid over thin needle with heat sink/source and Darcy–Forchheimer porous medium aspects. Arab J Sci Eng. 2020;45:9569–78.
[17] Hamid A, Khan M. Thermo-physical characteristics during the flow and heat transfer analysis of GO-nanoparticles adjacent to a continuously moving thin needle. Chin J Phys. 2020;64:227–40.
[18] Buongiorno J. Convective transport in nanofluids. J Heat Transf. 2006;128:240–50.
[19] Tiwari RK, Das MK. Heat transfer augmentation in a two-sided lid-driven differentially heated square cavity utilizing nanofluids. Int J Heat Mass Transf. 2007;50(9–10):2002–18.
[20] Nield DA, Kuznetsov AV. The Cheng-Minkowycz problem for natural convective boundary-layer flow in a porous medium saturated by a nanofluid. Int J Heat Mass Transf. 2009;52(25–26):5792–5.
[21] Kuznetsov AV, Nield DA. The Cheng-Minkowycz problem for natural convective boundary layer flow in a porous medium saturated by a nanofluid: A revised model. Int J Heat Mass Transf. 2013;65:682–5.
[22] Khan A, Shah Z, Alzahrani E, Islam S. Entropy generation and thermal analysis for rotary motion of hydromagnetic Casson nanofluid past a rotating cylinder with Joule heating effect. Int Commun Heat Mass Transf. 2020;119:104979.
[23] Islam S, Khan A, Kumam P, Alrabaiah H, Shah Z, Khan W, et al. Radiative mixed convection flow of maxwell nanofluid over a stretching cylinder with Joule heating and heat source/sink effects. Sci Rep. 2020;10:17823.
[24] Tlili I, Khan WA, Ramadan K. MHD flow of nanofluid flow across horizontal circular cylinder: steady forced convection. J Nanofluids. 2019;8(1):179–86.
[25] Khan WA, Aziz A, Uddin N. Buongiorno model for nanofluid Blasius flow with surface heat and mass fluxes. J Thermophys Heat Transf. 2013;27(1):134–41.
[26] Wakif A, Boulahia Z, Ali F, Eid MR, Sehaqui R. Numerical analysis of the unsteady natural convection MHD Couette nanofluid flow in the presence of thermal radiation using single and two-phase nanofluid models for Cu–water nanofluids. Int J Appl Comput Math. 2018;4(3):81.
[27] Rahman MM, Rosca AV, Pop I. Boundary layer flow of a nanofluid past a permeable exponentially shrinking surface with convective boundary condition using Buongiorno's model. Int J Numer Methods Heat Fluid Flow. 2015;25:299–319.
[28] Eid MR, Mahny KL. Unsteady MHD heat and mass transfer of a non-Newtonian nanofluid flow of a two-phase model over a permeable stretching wall with heat generation/absorption. Adv Powder Technol. 2017;28(11):3063–73.
[29] Kuznetsov AV. The onset of nanofluid bioconvection in a suspension containing both nanoparticles and gyrotactic microorganisms. Int Commun Heat Mass Transf. 2010;37:1421–5.
[30] Kuznetsov AV. Nanofluid bioconvection in water-based suspensions containing nanoparticles and oxytactic microorganisms: Oscillatory instability. Nanoscale Res Lett. 2011;6:100.
[31] Mallikarjuna B, Rashad AM, Chamkha AJ, Abdou M. Mixed bioconvection flow of a nanofluid containing gyrotactic

microorganisms past a vertical slender cylinder. Front Heat Mass Transf. 2018;10:21.
[32] Uddin MJ, Alginahi Y, Beg OA, Kabir MN. Numerical solutions for gyrotactic bioconvection in nanofluid-saturated porous media with Stefan blowing and multiple slip effects. Comput Math Appl. 2016;72:2562–81.
[33] Amirsom NA, Uddin MJ, Ismail AIM. MHD boundary layer bio-nanoconvective non-Newtonian flow past a needle with Stefan blowing. Heat Transf Asian Res. 2018;48:727–43.
[34] Khan WA, Rashad AM, Abdou M, Tlili I. Natural bioconvection flow of a nanofluid containing gyrotactic microorganisms about a truncated cone. Eur J Mech B Fluids. 2019;75:133–42.
[35] Waqas H, Hussain M, Alqarni MS, Eid MR, Muhammad T. Numerical simulation for magnetic dipole in bioconvection flow of Jeffrey nanofluid with swimming motile microorganisms. Waves Random Complex Media. 2021;1–18. doi: 10.1080/17455030.2021.1948634.
[36] Alwatban AM, Khan SU, Waqas H, Tlili I. Interaction of Wu's slip features in bioconvection of Eyring Powell nanoparticles with activation energy. Processes. 2019;7(11):859.
[37] Kumar A, Sugunamma V, Sandeep N, Jv RR. Impact of Brownian motion and thermophoresis on bioconvective flow of nanoliquids past a variable thickness surface with slip effects. Multidiscip Model Mater Struct. 2019;15(1):103–32.
[38] Akbar T, Batool S, Nawaz R, Zia QMZ. Magnetohydrodynamics flow of nanofluid due to stretching/shrinking surface with slip effect. Adv Mech Eng. 2017;9(12):1–11.
[39] Brown NM, Lai FC. Correlations for combined heat and mass transfer from an open cavity in a horizontal channel. Int Commun Heat Mass Transf. 2005;32(8):1000–8.
[40] Eastman JA, Choi SUS, Li S, Yu W, Thompson LJ. Anomalously increased effective thermal conductivities of ethylene glycol-based nanofluids containing copper nanoparticles. Appl Phys Lett. 2001;78(6):718–20.
[41] Khudheyer AF. MHD mixed convection in double lid-driven differentially heated trapezoidal cavity. Int J Appl Innov Eng Manag. 2015;4(2):100–7.
[42] Roy G, Nguyen CT, Lajoie PR. Numerical investigation of laminar flow and heat transfer in a radial flow cooling system with the use of nanofluids. Superlattices Microstruct. 2004;35(3–6):497–511.
[43] Kefayati GR, Gorji-Bandpy M, Sajjadi H, Ganji DD. Lattice Boltzmann simulation of MHD mixed convection in a lid-driven square cavity with linearly heated wall. Sci Iran. 2012;19(4):1053–65.
[44] Jamshed W, Eid MR, Hussain SM, Abderrahmane A, Safdar R, Younis O, et al. Physical specifications of MHD mixed convective of Ostwald-de Waele nanofluids in a vented-cavity with inner elliptic cylinder. Int Commun Heat Mass Transf. 2022;134:106038.
[45] Nadeem S, Hussain ST. Heat transfer analysis of Williamson fluid over exponentially stretching surface. Appl Math Mech (Engl Ed). 2014;35(4):489–502.
[46] Waheed MA. Mixed convective heat transfer in rectangular enclosures driven by a continuously moving horizontal plate. Int J Heat Mass Transf. 2009;52(21–22):5055–63.
[47] Acharya N, Bag R, Kundu PK. Unsteady Bioconvective Squeezing Flow with Higher-order Chemical Reaction and Second-order Slip Effects. Heat Transf. Sept. 2021;50(6):5538–62. doi: 10.1002/htj.22137
[48] Acharya N. Spectral quasi linearization simulation on the radiative nanofluid spraying over a permeable inclined spinning disk considering the existence of heat source/sink. Appl Math Comput. 2021:411:126547, doi: 10.1016/j.amc.2021.126547.
[49] Acharya N. Spectral quasi linearization simulation of radiative nanofluidic transport over a bended surface considering the effects of multiple convective conditions. Eur J Mech – B/Fluids. Nov. 2020;84:139–54. doi: 10.1016/j.euromechflu.2020.06.004.
[50] Shah Z, Saeed A, Khan I, Selim M, Ikramullah, Kumam P. Numerical modeling on hybrid nanofluid (Fe_3O_4 + MWCNT/H_2O) migration considering MHD effect over a porous cylinder. PLoS One. July 2021;16(7):e0251744. doi: 10.1371/journal.pone.0251744.
[51] Shah Z, Sheikholeslami M, Ikramullah, Kumam P. Simulation of entropy optimization and thermal behavior of nanofluid through the porous media. Int Commun Heat Mass Transf. Jan. 2021;120:105039. doi: 10.1016/j.icheatmasstransfer.2020.105039.
[52] Shah Z, Ikramullah, Kumam P, Selim MM, Alshehri A. Impact of nanoparticles shape and radiation on the behavior of nanofluid under the Lorentz forces. Case Stud Therm Eng. Aug. 2021;26:101161. doi: 10.1016/j.csite.2021.101161.
[53] Bilal M, Arshad H, Ramzan M, Shah Z, Kumam P. Unsteady hybrid-nanofluid flow comprising ferrous oxide and CNTs through porous horizontal channel with dilating/squeezing walls. Sci Rep. June 2021;11(1):12637. doi: 10.1038/s41598-021-91188-1.
[54] Marzougui S, Mebarek-Oudina F, Assia A, Magherbi M, Shah Z, Ramesh K. Entropy generation on magneto-convective flow of copper–water nanofluid in a cavity with chamfers. J Therm Anal Calorim. Feb. 2021;143(3):2203–14. doi: 10.1007/s10973-020-09662-3.
[55] Daftardar-Gejji V, Jafari H. An iterative method for solving nonlinear functional equations. J Math Anal Appl. 2006;316(2):753–63.
[56] Daftardar-Gejji V, Bhalekar S. Solving fractional boundary value problems with Dirichlet boundary conditions using a new iterative method. Comput Math Appl. 2010;59(5):1801–9.
[57] Daftardar-Gejji V, Bhalekar S. Solving fractional diffusion-wave equations using a new iterative method. Fract Calc Appl Anal. 2008;11(2):193–202.
[58] Bhalekar S, Daftardar-Gejji V. Solving fractional-order logistic equation using a new iterative method. Int J Differ Equ. 2012;2012:1–12. doi: 10.1155/2012/975829.
[59] Bhalekar S, Daftardar-Gejji V. Convergence of the new iterative method. Int J Differ Equ. 2011;2011:1–10. doi: 10.1155/2011/989065.
[60] Hemeda AA. New iterative method: application to nth-order integro-differential equations. Int Math Forum. 2012;7(47):2317–32.
[61] Yaseen M, Samraiz M. A modified new iterative method for solving linear and nonlinear Klein-Gordon Equations. Appl Math Sci. 2012;6:2979–87.
[62] Patade J, Bhalekar S. Approximate analytical solutions of Newell-Whitehead-Segel equation using a new iterative method. World J Model Simul. 2015;11(2):94–103.
[63] Noor KI, Noor MA. Iterative methods with fourth-order convergence for nonlinear equations. Appl Math Comput. 2007;189(1):221–7.

[64] Noor MA, Waseem M, Noor KI. New iterative technique for solving a system of nonlinear equations. Appl Math Comput. 2015;271:446–66.

[65] Shah FA, Noor MA. Higher order iterative schemes for nonlinear equations using decomposition technique. Appl MathComput. 2015;266:414–23.